



저작자표시-비영리-변경금지 2.0 대한민국

이용자는 아래의 조건을 따르는 경우에 한하여 자유롭게

- 이 저작물을 복제, 배포, 전송, 전시, 공연 및 방송할 수 있습니다.

다음과 같은 조건을 따라야 합니다:



저작자표시. 귀하는 원저작자를 표시하여야 합니다.



비영리. 귀하는 이 저작물을 영리 목적으로 이용할 수 없습니다.



변경금지. 귀하는 이 저작물을 개작, 변형 또는 가공할 수 없습니다.

- 귀하는, 이 저작물의 재이용이나 배포의 경우, 이 저작물에 적용된 이용허락조건을 명확하게 나타내어야 합니다.
- 저작권자로부터 별도의 허가를 받으면 이러한 조건들은 적용되지 않습니다.

저작권법에 따른 이용자의 권리는 위의 내용에 의하여 영향을 받지 않습니다.

이것은 [이용허락규약\(Legal Code\)](#)을 이해하기 쉽게 요약한 것입니다.

[Disclaimer](#)

Thesis for the Degree of
Master of Engineering

Study on Needle Hydrophone for Low Frequency Photoacoustic Imaging

by

Xiaofeng Fan

Department of Interdisciplinary Program of Biomedical Mechanical

& Electrical Engineering

The Graduate School

Pukyong National University

August 2015

Study on Needle Hydrophone for Low Frequency Photoacoustic Imaging

Advisor: Prof. Junghwan Oh

by

Xiaofeng Fan

A thesis submitted in partial fulfillment of the requirements
for the degree of
Master of Engineering

in Department of
Interdisciplinary Program of Biomedical Mechanical & Electrical Engineering
The Graduate School
Pukyong National University

August 2015

**Study on Needle Hydrophone for
Low Frequency Photoacoustic Imaging**

A dissertation

by

Xiaofeng Fan

Approved by:



(Chairman) Hyun-Wook Kang



(Member) Seung-Yun Nam



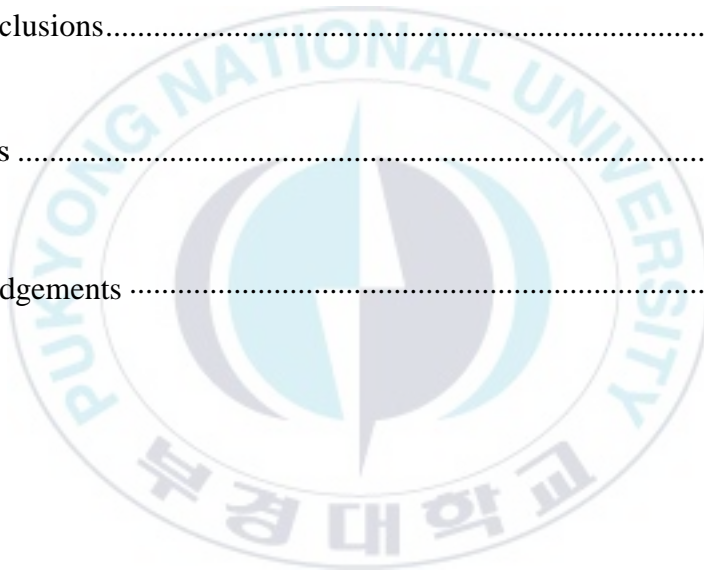
(Member) Junghwan Oh

May 18, 2015

Contents

Abstract	6
Ch. 1. Introduction.....	8
1.1 Backgrounds.....	8
1.2 Purposes	10
Ch. 2. Piezoelectric materials and Photoacoustic imaging (PAI)	12
2.1 Piezoelectric materials for needle hydrophones.....	12
2.1.1 Piezoelectric polymers	13
2.1.2 Piezoelectric ceramics	14
2.1.3 Piezoelectric single crystals	15
2.2 Photoacoustic Imaging(PAI)	18
2.3 Needle hyrophones for photoacoustic imaging (PAI)	21
Ch.3. Design and simulation of needle hyrophones for PAI	23
3.1 Simulation anddesign	24
3.1.1 Simulation	24
3.1.2 Design	28
Ch.4. Fabrication and charaterisits evaluation of needle hyrophones	30
4.1 Fabrication.....	30
4.2 Charaterisits evaluation	32
4.2.1 Receiving Pulse-echo response	32

4.2.2 Discussion	40
Ch.5. Photoacoustic imaging by the fabricated needle hydrophone.....	42
5.1 Photoacoustic imaging system	42
5.1.1 Indocyanine green (ICG) specimen.....	42
5.1.2 Photoacoustic imaging setup.....	43
5.2 Photoacoustic imaging results.....	45
Ch.6. Conclusions.....	49
References	51
Acknowledgements	57



List of Tables

Table 2-1 Physical properties of piezoelectric single crystals.....	16
Table 3-1. Comparison of the material properties between PVDF and PMN-PZT.	24
Table 4-1. Acoustic parameters of the matching layers used in fabrication.	31

List of Figures

Fig.2-1. Principle of photoacoustic imaging.	19
Fig.2-2. Schematics of photoacoustic tomography (a) and (b).....	20
Fig.3-1. PMN-PZT single crystals used to fabricate the needle hydrophone... ..	23
Fig.3-2. Simulated receiving impulse responses of PMN-PZT needle hydrophones.....	25
Fig.3-3. Simulated receiving impulse responses of PVDF needle hydrophones.	26
Fig.3-4. Simulated receiving impulse responses of PMN-PZT and PVDF needle hydrophones (time domain).....	27
Fig.3-5. Simulated receiving impulse responses of PMN-PZT and PVDF needle hydrophones (frequency domain).	28

Fig.3-6. Structure of the PMN-PZT needle-type hydrophone.....	29
Fig.4-1. Schematic diagram of the setup for evaluation of the PMN-PZT needle hydrophone.	33
Fig. 4-2. xyz rectangular coordinate system and the transducer.	34
Fig.4-3. Wave graphs of the PMN-PZT without and with two matching layers (Attenuation=0, Gain=20dB).....	35
Fig.4-4. Wave graph of the PMN-PZT needle hydrophone without an amplifier	36
Fig.4-5. Wave graph of the PMN-PZT needle hydrophone with an amplifier	36
Fig.4-6. Mini-circuit ZFL-500-BNC amplifier.....	37
Fig.4-7. Wave graph of the PVDF needle hydrophone with amplifier.....	38
Fig.4-8. Comparison of waveform of typical signals for the PMN-PZT and PVDF needle hydrophones. (Attenuation=0, Gain=8dB).....	38
Fig.4-9. Comparison of amplitude variation according to frequency for the PMN-PZT and PVDF needle hydrophones. (Attenuation=0, Gain=8dB).....	39
Fig.4-10. Photograph of the fabricated PMN-PZT needle hydrophone	40
Fig.5-1. ICG specimen.....	43
Fig.5-2. PAI system	44
Fig.5-3. PA signal of PMN-PZT needle hydrophone without amplifier.....	45
Fig.5-4. PA signal of PMN-PZT needle hydrophone with an amplifier (Gain=20dB).....	45

Fig.5-5. PA signal of PVDF needle hydrophone with an amplifier (Gain=34dB).....	46
Fig.5-6. PA image of ICG specimen.....	47
Fig.5-7. PA image of human hair specimen.....	48



Study on Needle Hydrophone for Low Frequency Photoacoustic Imaging

Xiaofeng Fan

Department of
Interdisciplinary Program of Biomedical Mechanical & Electrical Engineering
The Graduate School,
Pukyong National University



Abstract

The low frequency photoacoustic imaging system usually uses several MHz ultrasound signals. In order to detect the signals, several kinds of ultrasound transducers including needle hydrophones have been developed so far. However, the sensitivity and frequency bandwidth of those transducers are still not enough to detect very small photoacoustic signals from specimen with low thermoelastic effect, such as biological tissues.

In this paper, a design and fabrication of a new type of needle hydrophone with high sensitivity and wide bandwidth in the range of 1~10 MHz is described in detail. The piezoelectric material of the hydrophone is lead magnesium niobate-lead titanate (PMN-PZT) which has very high electromechanical coupling coefficient (> 0.9). The sensing part of the hydrophone is small

(0.5x0.5 mm²) and has two matching layers on the tip of the needle. Construction and performance are compared with other types of needle hydrophones. The receiving frequency responses of the hydrophones are simulated by the PiezoCAD program based on the KLM equivalent circuit model. It was characterized to be more sensitive than PVDF needle hydrophones of the similar structure, and it was confirmed by experiment. Furthermore an Acoustic Needle Imaging System for low frequency photoacoustic imaging was established using this fabricated PMN-PZT needle hydrophone to get some images of specimens. The images of the ICG specimen and human hair obtained by the established system have high resolution and high contrast. Conclusively, it is shown that the hydrophone is very useful in photoacoustic imaging.



Ch. 1. Introduction

1-1. Backgrounds

In recent years, diagnostic and therapeutic ultrasound is widely used in physical inspection and treatment of diseases, such as lithiasis and some kinds of cancers [1]. In the usage, the ultrasound is generated by a transducer which is usually made by piezoelectric materials, and it forms an acoustic field in medium of human body. Occasionally, the intensity of the field is very high and harmful so that the requirements of quantitative measurement of the spatial and temporal characteristics of the field are increasing. The requirements promote the development of a good needle hydrophone with high sensitivity and wide bandwidth.

A needle hydrophone is designed adequately through the simulation of receiving sensitivity for desired fields of application, such as medical imaging, and it is made by using piezoelectric materials. The piezoelectric materials are classified by three kinds, such as single crystal, ploy crystal and polymer materials. So far, piezoelectric polymer of Polyvinylidene fluoride PVDF and its copolymer of poly(vinylidenefluoride-co-trifluoroethylene) P(VDF-TrFE) are widely used as sensing materials for the hydrophone in the frequency range over 1 MHz. They have similar acoustic impedances with water or biological tissues and low mechanical quality factors so that they are useful to make a wideband transducer as well as a hydrophone without any matching layer. However, their electromechanical coupling factors are too low (< 0.3) to make a high sensitive transducer [2].

The PZT stands for the piezoelectric poly crystalline material. It has not only relatively high electromechanical coupling coefficient (~ 0.6) and high permeability, but also very good stability on temperature variation. And, it is easy to make various type transducers by using the PZT because of its good machinability. It has been most widely used as the piezoelectric material of ultrasound transducer until the relaxor-based piezoelectric single crystal was developed in 1980s.

The piezoelectric single crystal of PZN-PT ($\text{Pb}(\text{Zn}_{1/3}\text{Nb}_{2/3})\text{O}_3\text{-xPbTiO}_3$) and PMN-PT ($\text{Pb}(\text{Mg}_{1/3}\text{Nb}_{2/3})\text{O}_3\text{-PbTiO}_3$) was developed on 1981 and 1989, respectively [3, 4]. These single crystals have extremely high electromechanical coupling coefficients (> 0.9). It means the electromechanical energy conversion efficiency is higher than 80 %. Recently, there is a trend towards the use of this single crystal to fabricate high performance ultrasound transducers. Thereafter, some modified piezoelectric single crystals, such as lead magnesium niobate-lead titanate PMN-PZT($(1-x) \text{Pb} (\text{Mg}_{1/3}\text{Nb}_{2/3}) \text{O}_3\text{-xPb} (\text{Zr}_{0.53},\text{Ti}_{0.47}) \text{O}_3$) have been developed by changing the composition of relaxor [5, 6].

On the other hand, photoacoustic imaging (PAI) has the potential to image animal or human organs, such as the breast and the brain, with high spatial resolution and high contrast [7, 8]. The photoacoustic (PA) or optoacoustic effect is the physical basis of the imaging. It refers to the generation of acoustic waves by absorption of electromagnetic energy of light. In order to obtain this effect the light intensity must vary, either periodically (modulated light) or as a single flash (pulsed light). Alexander Graham Bell first reported the observation of sound generated by light in 1880 [9]. In the last decade, works on PAI have demonstrated many valuable achievements in the fields of biomedical

application [10, 11]. Non-ionizing waves, such as short laser pulses, are often used to excite ultrasound waves which is called as PA signals.

PAI systems are classified by photoacoustic microscope (PAM) and photoacoustic tomography (PAT). The frequency of the PA signal for the system is between several MHz and about one hundred MHz. Conventional PAI systems, especially conventional PAMs, use several MHz PA signals. Here, it is called as a low frequency PAI system.

In order to obtain the PA images with high resolution and high contrast, the ultrasound transducer or needle hydrophones to detect the PA signals should have high sensitivity and wide frequency bandwidth. Taking into consideration of the characteristics, the PMN-PZT could be a candidate material to design and fabricate a needle hydrophone with high sensitivity for the low frequency PAI.

1-2. Purposes

The first purpose of this study is to design and fabricate a needle hydrophone with high sensitivity in the range of 1~10 MHz. For the purpose, the single crystal PMN-PZT is used as piezoelectric material and two matching layers are selected through the computer simulation of receiving impulse sensitivity. A copper (Cu) wire is used as its backing material. The size of the sensing area is $0.5 \times 0.5 \text{ mm}^2$. The design and fabrication method of this miniature hydrophone is developed and described in this paper. The characteristics of the fabricated hydrophone are confirmed by comparison of the performances with a commercialized hydrophone.

The second is to establish a PA system for obtaining images of specimens

including biological tissues by using the fabricated needle hydrophone. Here, it is called as the Acoustic Needle Imaging System for low frequency photoacoustic imaging. Using the system, the images of the ICG specimen and human hair are obtained.



Ch. 2. Piezoelectric materials and photoacoustic imaging (PAI)

2-1. Piezoelectric materials for needle hydrophones

In order to have good performances, the needle hydrophone is required to have high, stable, and flat sensitivity over a wide bandwidth and also have high signal-to-noise ratio (SNR) and a suitable size for giving spatial resolution [12]. For these concerns, a couple of properties of the piezoelectric materials used to fabricate needle hydrophones are required and they can be summarized as follows: First, to obtain high sensitivity, the piezoelectric materials should have high piezoelectric constants. Second, high dielectric constants are needed to make it much easier for electrical matching with impedance. Third, in order to get low noise generation, the material should have low dielectric loss [13, 14, 15].

The piezoelectric materials have electric charges which are accumulated in response to applied mechanical strain and vice versa, it is deformed under the external electric field. The electromechanical effect, which is called piezoelectricity, is intimately related to the crystallographic structure of the materials and it cannot exist in the materials with the center of symmetry. Since Pierre Curie and Jacques Curie [16] firstly demonstrated the piezoelectricity in 1880, many piezoelectric materials have been discovered. Those are classified by three kinds, such as polymer, ceramic and single crystal, and each kind of them contains plenty of specific materials and properties.

2-1-1. Piezoelectric polymers

Several kinds of crystallized Polymers such as PVDF, P(VDF-TrFE), Polyvinylidene Fluoride-Tetrafluoroethylene (P(VDF-TeFE)) and nylon have piezoelectricity. Those materials are called piezoelectric polymer or piezoelectric copolymer. These kinds of materials are flexible and have low density, low acoustic impedance and relatively high piezoelectric constants. Due to these advantages, piezoelectric polymers attract worldwide attentions and they are applied widely in development of ultrasound transducers. Besides, the piezoelectric polymers have been used to make pressure sensors (strain sensor), electrets-microphones, tactile sensors and so on.

In 1969, Kawai and his colleague Fukada reported the discovery of a large remnant polarization in oriented films of PVDF [17]. Since the discovery, many new piezoelectric and ferroelectric polymers have been studied in great detail [18, 19]. The PVDF film can be obtained from the melt solution. But this kind of PVDF is non-polarized α -phase form. To be rendered piezoelectric, it should be converted to the polarized β -phase form by stretching the film into approximately 4 to 5 times of its original lateral dimensions. Because the stretching cannot convert all of the α -phase to β -phase, the obtained PVDF film is composite-like in structure with both α and β phases. Nowadays, both uniaxially stretched and biaxially stretched piezoelectric PVDF films are commercially available, and have been used successfully for high frequency ultrasonic devices [20].

Ferroelectric copolymers of PVDF, which can possess significantly higher remnant polarization than PVDF, were discovered in the 1980s. The P(VDF-TrFE), P(VDF-TeFE) and P(VDF-TrFE-CFE) are the available piezoelectric

copolymers which have been studied and reported extensively. Among them, P(VDF-TrFE) is the most successful commercial ferroelectric copolymer because of its superior piezoelectric properties. Although other piezoelectric polymer materials remain under investigation for their feasibility for high frequency acoustic devices, none of them can achieve the same piezoelectric properties as commercially available PVDF or P(VDF-TrFE).

2-1-2. Piezoelectric ceramics

Piezoelectric ceramics are multi-crystalline ferroelectric materials with high dielectric constants. Lead Zirconate Titanate (PZT), Barium Titanate (BT), Lead Titanate (PT) and Lead Metaniobate (PN) are the usual piezoelectric ceramics. The piezoelectric ceramics have strong piezoelectricity and can readily be cut into various sizes and shapes. However, their small mechanical quality factor, high electric loss and poor stability were the disadvantages in the early stage.

Between 1941 and 1947, a series of studies on barium oxide-titanium oxide compositions conducted independently in the USA, the USSR and Japan. Most of their studies conclude the discovery of good piezoelectric properties of poled ferroelectric Barium Titanate (BaTiO_3) ceramic. This was the beginning of the remarkable development in polycrystalline ceramic materials which has continued to the present days. Its basic characteristic is the ferroelectricity of the single crystals consisted in the polycrystalline. By applying an external electrical field, the spontaneous electric moment in the crystal can orient to a preferred direction. This process makes the ferroelectric material become piezoelectric. In addition, this material presents a high dielectric constant, which results in a low

electrical impedance, generally useful for ultrasonic transducer. This discovery opened up the field of piezoelectric ceramics and their application to ultrasound transducer. After BaTiO_3 , PZT was found by Jaffet et al. [21] in 1954. The PZT marked a milestone in the development of piezoelectric ceramics because of the strong and stable piezoelectric characteristics. Thereafter the PZT and its related materials have constituted the domain piezoceramics and have been used most widely in ultrasonic transducers.

2-1-3. Piezoelectric single crystals

The piezoelectric single crystals include Quartz (SiO_2), Lithium Niobate (LiNbO_3), Zinc oxide (ZnO), and Lead Magnesium Niobate-Lead Titanate (PMN-PT), Lead Zinc Niobate-Lead Titanate (PZN-PT), lead magnesium niobate-lead titanate (PMN-PZT) and so on. Table 1-1 shows their physical properties. The PMN in PMN-PT and the PZN in PZN-PT role as relaxors so that they are called as relaxor-based piezoelectric single crystals.

The SiO_2 is one of the most widely used piezoelectric single crystals for oscillators, and it belongs to crystal class 32 (or D3). During the World War I , people made the first transducer by a thin SiO_2 crystal plate, and it was the main piezoelectric material in the next several years.

The ferroelectric property of LiNbO_3 was first discovered in 1949 [22]. It was synthesized into single crystal form and its property was investigated in detail at Bell Laboratory [23]. The LiNbO_3 belongs to a trigonal crystal group ($R3c$) and it has large piezoelectric, pyroelectric and photoelectric coefficients. It is well known as piezoelectric material in surface acoustic wave (SAW) devices for use as delay lines, filters, and ultrasound transducers. Knapik et al.

used a 15-30 μm thickness LiNbO_3 single crystals to make the transducers which could provide resonances in the range from 100 to 200 MHz successfully [24]. Nowadays, due to the advanced synthesis method and dicing technology, it is possible to obtain the nano-scale LiNbO_3 single crystals to make ultra-high frequency (UHF) transducers.

Table 2-1. Physical properties of piezoelectric single crystals [25-29]

Parameters	LiNbO_3	SiO_2	PMN-PT	ZnO	PZN-PT	PMN-PZT
Density: ρ (g/cm^3)	4.64	2.65	8.00	6.33	8.35	7.35
Longitudinal velocity: v_l (km/s)	7.34	5.97	4.61	5.68	1.06	4.25
Relative permittivity: ϵ_r	39.0	3.75	797	10.2	1000	1030
Mechanical quality factor: Q_m	10000	2000	31.0	1500	39.5	100
Electromechanical coupling coefficient: k_t	0.49	0.09	0.58	0.28	0.53	0.62
Curie temperature: T_c ($^\circ\text{C}$)	1150	573	131	≥ 27	160	216

High quality single crystal ZnO film is required for many applications, such as in acoustic microscope, SAW device, photoluminescence and so on. Because of high electromechanical coupling coefficient and low insertion loss, Ito et al. made a 100-MHz ultrasound linear transducer array by using a 10 μm thick ZnO film sputtered on a sapphire substrate [30]. Martin et al. deposited Aluminum Nitride (AlNO_3) and ZnO thin film by reactive magnetron sputtering and made the ultrasound transducer in 100-300 MHz range [31].

The relaxor-based piezoelectric single crystals are most recently developed. The PMN-PT and PZN-PT single crystals with the ultrahigh longitudinal

piezoelectric strain coefficient d_{33} (>2000 pC/N) and electromechanical coupling factors k_{33} (>0.9) suggest higher sensitivity, wider bandwidth and higher source level in ultrasonic transducer applications. These merits are promising for a broad range of electromechanical applications.

With the outstanding electrical properties, the PMN-PT single crystal has been used as the active element of high frequency bio-medical sensors and transducers. S.T.LAU designed a piezoelectric PMN-PT fiber hydrophone for ultrasonic transducer calibration with the element size as small as 0.25mm in diameter [32]. And Qifa Zhou fabricated a high frequency PMN-PZT ultrasonic needle transducers for pulsed-wave Doppler application [33].

Single crystals of the PZN-PT have been investigated to improve device performance through increased electromechanical coupling and decreased acoustic impedance. Kuwata et al. observed the k_{33} values and reported the ultra-high electromechanical coupling coefficient of PZN-PT single crystals by [34]. Modeled bandwidths of over 120% were predicted for array transducers incorporating these materials. Saitoh et al. in 1998 demonstrated improved performance and superior imaging with 128 channel phased array probes incorporating PZN-PT single crystals [35].

The PMN-PZT single crystals is a promising candidate for applications in electronic and microelectronic devices. It exhibits a high dielectric constant, high electromechanical coupling coefficient, low sintering temperature and a broad dielectric maximum just below room temperature [36]. Its excellent dielectric and piezoelectric properties make them the best candidates for transducers, actuators, and single crystal-polymer composites.

Although piezoelectric single crystals have very good stability and high

mechanical quality factors, they are fragile and the dielectric constant is not enough to generate high power acoustic waves. So, piezoelectric single crystal materials are usually used to make standard frequency control oscillators or high selective SAW filters with narrow frequency band.

2-2. Photoacoustic Imaging (PAI)

PAI is also called optoacoustic or thermoacoustic imaging. In PAI, acoustic transient waves, that is photoacoustic waves, are generated by using pulsed laser radiation. The photoacoustic waves are then detected by a transducer, such as a needle hydrophone, and used to form an image of spatial distribution of optical absorption. Such absorption leads to local heating and thermoelastic expansion, which can produce megahertz ultrasonic waves in materials. Since different biological tissues have different absorption coefficient, by measuring the acoustic signals with ultrasonic transducers, one can rebuild the distribution of optical energy deposition and ultimately obtain images of the biological tissues.

The PAI is a non-invasive imaging modality which allows structural, functional and molecular imaging. The method relies on the PA effect which is conversion between light and acoustic waves due to absorption of electromagnetic waves and localized thermal excitation. The principle is depicted in Fig. 2-1. Short pulses of electromagnetic radiation, mostly short laser pulses, are used to illuminate a sample. The local absorption of the light is followed by rapid heating, which subsequently leads to thermal expansion. Finally, broadband acoustic waves with short duration are generated. By recording the propagating ultrasonic waves with adequate ultrasonic transducers

at outside of the sample, the initial absorbed energy distribution can be calculated and then an image is reconstructed. Thus, PAI is a hybrid technique using the effects of optical absorption and ultrasonic wave propagation. Thereby the advantages of both techniques related to the two effects are combined to give the high contrast of optical imaging and the high resolution of ultrasonic imaging.

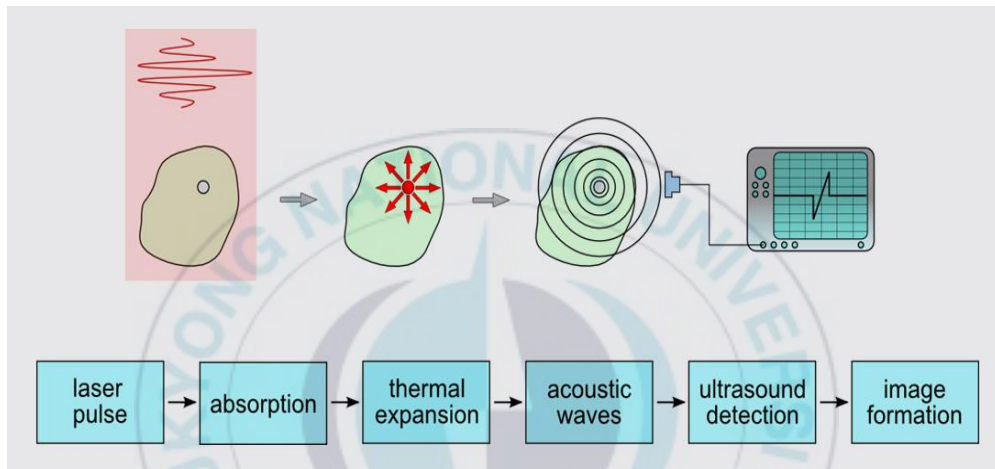


Fig. 2-1. Principle of photoacoustic imaging.

It is known that optical absorption is closely associated with physiological properties, such as hemoglobin concentration and oxygen saturation. As a result, the magnitude of the ultrasonic emission (i.e. photoacoustic signal), which is proportional to the local energy deposition, reveals physiologically specific optical absorption contrast. 2D or 3D images of the targeted areas can then be formed.

In the last decade, works on PAI have demonstrated many valuable achievements in biomedical applications [37]. Possessing many attractive characteristics such as the use of non-ionizing electromagnetic waves, good

resolution/contrast, portable instrumentation, as well as the ability to quantitate the signal to a certain extent, photoacoustic techniques have been applied for the imaging of cancer, wound healing, disorders in the brain, gene expression, among others. As a promising structural, functional and molecular imaging modality for a wide range of biomedical applications, photoacoustic imaging systems can be briefly categorized into two types: photoacoustic tomography (PAT) and photoacoustic microscopy (PAM).

In PAT a semitransparent sample is illuminated by an expanded laser beam, thus illuminating the whole sample volume (Fig. 2-2(a)). The spatial varying local absorption leads to generation of ultrasonic waves which are recorded by an ultrasonic transducer (Fig. 2-2(b)). By moving the transducer around the sample, or by using an array of transducers, a dataset of pressure curves is acquired. By using adequate reconstruction algorithms the absorption of light within the sample (that is, image information) can be reconstructed. The resolution of PAT is determined by the duration of the excitation laser pulse and the bandwidth of the transducers, and is typically below 100 μm .

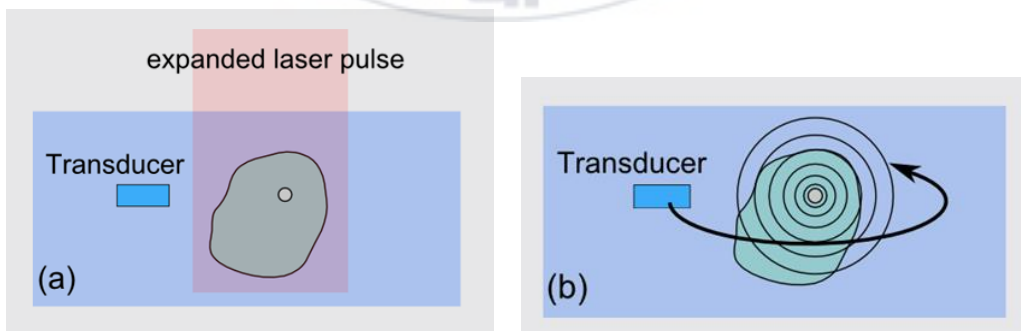


Fig. 2-2. Schematics of photoacoustic tomography (a and b)

Optical waves, instead of electromagnetic waves at other wavelengths, are used in photoacoustic imaging because of their desirable physical properties such as deeper tissue penetration and better absorption by contrast agents. The combination of high ultrasonic resolution with good image contrast due to optical absorption is quite advantageous for imaging purposes [38]. When compared with optical imaging, in which the scattering in tissues limits the spatial resolution with increasing depth, PAI has higher spatial resolution and deeper imaging depth since scattering of the ultrasonic signal in tissue is much weaker. When compared with ultrasound imaging, in which the contrast is limited due to the mechanical properties of biological tissues, PAI has better contrast which is related to the optical properties of different tissues. In addition, the absence of ionizing radiation also makes PAI safer than other imaging techniques such as computed tomography and radionuclide-based imaging techniques.

Given that optical absorption can reveal various physiological parameters such as hemoglobin, melanin, water, ion concentration and oxygen saturation in living subjects, PAI is a promising structural, functional and molecular imaging modality for a wide range of biomedical applications.

2-3. Needle hydrophones for photoacoustic imaging (PAI)

In PAI, three steps are included to obtain an image: laser pulses illuminate a sample, ultrasound transducers detect the acoustic waves and data processing for image construction. Among the three steps, detecting the acoustic waves is of much more importance, and the resolution and quality of the constructed

image is associated with the performance and characteristics of the ultrasound transducer. Thus, only with high sensitivity and broad bandwidth of the transducer can build a good PAI system.

The most often used ultrasound detectors in PAI are piezoelectric based. They have low thermal noise and high sensitivity and can provide a wide band of up to 100 MHz. YANG Di-Wu obtained PA images of animals with an annular transducer array whose central frequency and bandwidth are 7.5MHz and 75%, respectively [39]. And Diwu Yang established a fast full-view PAI system by combined scanning with a linear transducer array of 7.5 MHz resonance frequency [40]. Shriram Sethuraman established an intravascular PAI system by using a single-element, high-frequency (40 MHz), unfocused intravascular ultrasound imaging catheter (2.5 F, 0.83-mm diameter) [41].

Generally, the ultrasound transducers used for PAI are divided into high frequency range (> 30 MHz) and low frequency range (< 30 MHz). In this study, the low frequency (lower than 10 MHz) transducers are focused. In order to get high sensitivity and broad bandwidth of the transducer, a new piezoelectric single crystal PMN-PZT as the sensing material is selected.

Ch. 3. Design and simulation of needle hydrophones for PAI

In this experiment, piezoelectric single crystal PMN-PZT (Ceracomp Co., Ltd.) was used as the sensing material of the needle hydrophone. Fig.3-1 shows the plates of the PMN-PZT single crystal with the size of $0.5 \times 0.5 \text{ mm}^2$. Compared with conventional piezoelectric materials, such as PVDF, which has long been used as the sensing material of hydrophones, the single crystal PMN-PZT has several advantages. For example, PMN-PZT has ultra-high piezoelectric properties. Needle hydrophones made of PMN-PZT especially have high sensitivity in the frequency range of 1~10 MHz. Its excellent dielectric and piezoelectric properties make them the best candidates for transducers, actuators, and single crystal-polymer composites.

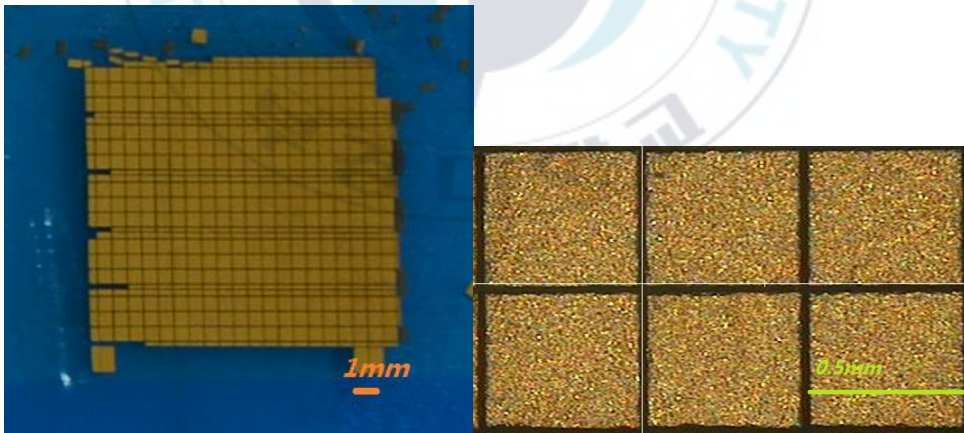


Fig.3-1. PMN-PZT single crystals used to fabricate the needle hydrophone

Table 3-1 shows the comparison of the material properties between PVDF and PMN-PZT. Because of small acoustic impedance of PVDF, the matching

layer is not necessary for water or biological tissues. However, compared with water or biological tissue, the acoustic impedance of the PMN-PZT is much higher. Thus, in order to reduce the interface reflection of sound waves, one or two matching layers are required.

Table 3-1. Comparison of the material properties between PVDF and PMN-PZT.

	PMN-PZT	PVDF
K_t	0.62	0.2
$\epsilon_{33}^S/\epsilon_0$	1030	11
α [dB/mm/MHz]	0.01	0.5
V^D [m/s]	4249	2200
ρ [kg/m ³]	7350	1800
Z [Mrayl]	31.2	3.96

3-1. Simulation and Design

3-1-1. Simulation

The piezoelectric single crystal PMN-PZT needle hydrophone was designed using the one-dimensional Krimholtz-Leedom-Matthae (KLM) model software PiezoCAD (Version 3.03 for Windows, Sonic concepts, Wood-in-ville, WA). Three main components are involved including active element, backing layer and matching layer. The single crystal PMN-PZT with an active area of

0.5×0.5 mm² and a thickness of 0.31 mm was used as the active element of the needle hydrophone. In the design, we considered the structure of Cu (41.6 Mrayl) backing and two matching layers (Comico_11 and Comico_10, KoMiCo company) bonded together with the PMN-PZT plate for the needle hydrophone. The two matching layers were bonded together onto the front surface of the needle hydrophone with the single crystal PMN-PZT active element by using the conductive silver epoxy (EPO-TEK H20). According to DeSilets et al. [42], the acoustic impedance of the matching layer is $Z_1 = 8.49$ Mrayl, $Z_2 = 2.31$ Mrayl, for the thickness of $\lambda/4$ (λ is the wavelength), respectively.

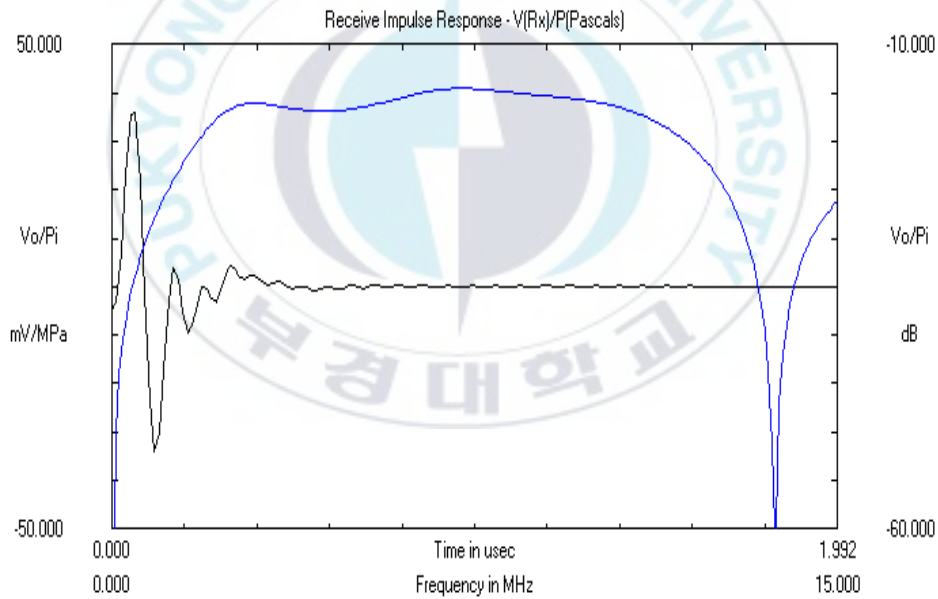


Fig.3-2. Simulated receiving impulse responses of PMN-PZT needle hydrophones

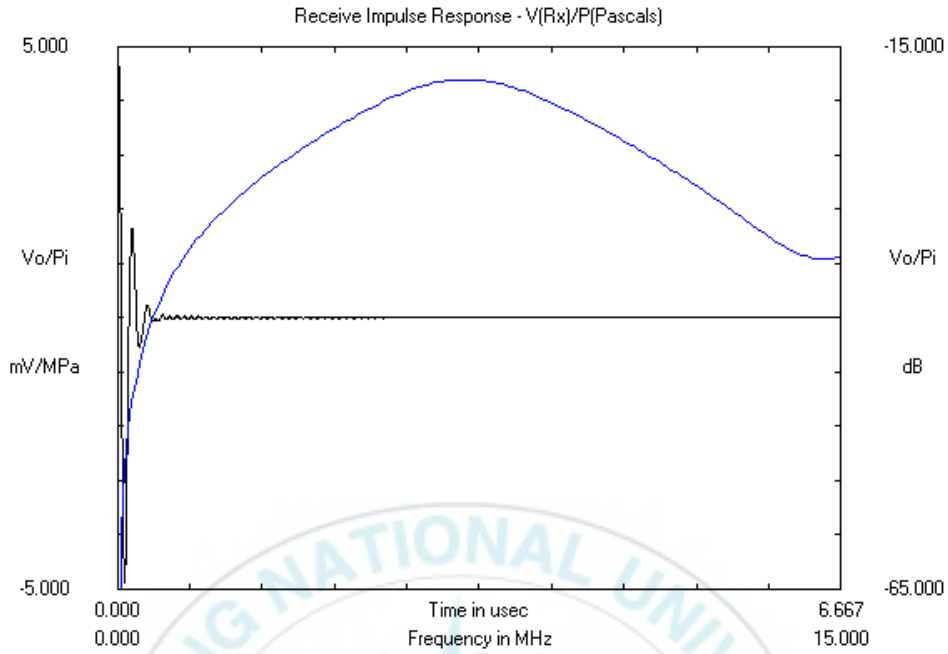


Fig.3-3. Simulated receiving impulse responses of PVDF needle hydrophones

Fig.3-2 and Fig.3-3 show the simulated receiving impulse of PMN-PZT and PVDF needle hydrophones. In order to compare the differences of the simulated receiving impulse responses of these two different kinds of needle hydrophones, Fig.3-4 and Fig.3-5 clearly shows the comparison of receiving impulse response and spectrum between PMN-PZT and PVDF needle hydrophones. Here, the thickness of sensing material PVDF is $80 \mu\text{m}$, which was calculated corresponding to the thickness of PMN-PZT plate. As shown in Fig.3-4, the voltage of the received signal by the PMN-PZT needle hydrophone is about 37 mV at the peak value which is More than 7 times higher than that received by the standard commercial PVDF needle hydrophone which is about 5 mV at the peak value. Also, in the frequency domain, as shown in Fig.3-5, the PMN-PZT

needle hydrophone shows more flat and wider bandwidth in the frequency range of 0~13 MHz. These simulated results fully illustrated the potential excellent performances of the PMN-PZT needle hydrophone and that needle hydrophones made of PMN-PZT especially have high sensitivity and stability in the frequency range of 1~10 MHz.

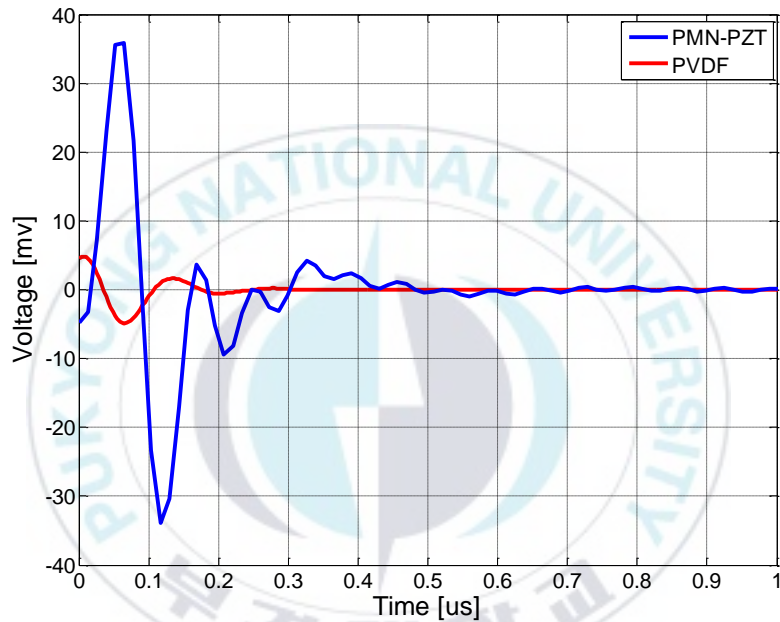


Fig.3-4. Simulated receiving impulse responses of PMN-PZT and PVDF needle hydrophones (time domain)

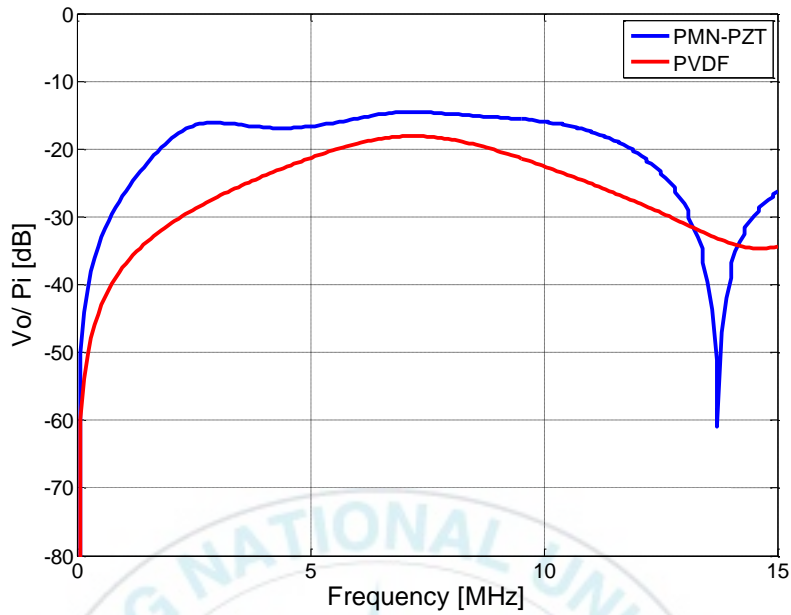


Fig.3-5. Simulated receiving impulse responses of PMN-PZT and PVDF needle hydrophones (frequency domain)

3-1-2. Design

Fig.3-6 shows the structure of the PMN-PZT needle hydrophone. The size of the rectangular single crystal PMN-PZT plate is $0.5 \times 0.5 \text{ mm}^2$ in area and a thickness of 0.31 mm. Two matching layers (0.063 mm and 0.05 mm in thickness, respectively), which were used to reduce the interface reflection of sound waves and improve the sensitivity of the PMN-PZT needle hydrophone, were bonded in front of the single crystal PMN-PZT plate. The copper (Cu) wire ($\Phi \approx 0.7 \text{ mm}$) which was coated with Teflon and inserted into the stainless iron tube is used as the baking layer of the needle hydrophone. The Teflon ensured that the iron tube and copper wire were separated from each other, thus making them to be the two electrodes of the needle hydrophone.

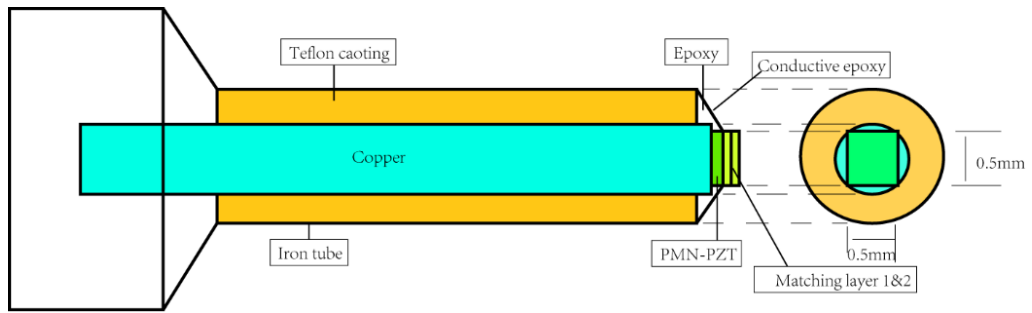


Fig.3-6 Structure of the PMN-PZT needle-type hydrophone



Ch. 4. Fabrication and characteristics evaluation of needle hydrophones

4-1. Fabrication

In our experiment we selected the main part of the hypodermic needle (1mm in diameter) as the tube of the needle hydrophone. We cut the tip and end of the hypodermic needle first, thus making it to be an iron tube only. And then polished the two sides of the iron tube and made them plane. The copper wire, which was coated with Teflon ahead of time and polished flat in the surface of one end, was inserted into the iron tube slowly. The copper wire is about 2 or 3mm longer than the iron tube at one end (called end A). The Teflon ensured that the iron tube and copper wire were separated from each other, thus both of them would be the positive and negative electrodes of the needle hydrophone. In order to make the copper and the iron tube to be a unit, an adhesive layer of non-conductive epoxy (EPO-TEK 301) was used to bond them together at the interfaces.

One surface of the piezoelectric single crystal PMN-PZT plate (thickness of 0.31mm, and $0.5 \times 0.5 \text{ mm}^2$ in area) was bonded together with the copper wire at end A by using the conductive silver epoxy (EPO-TEK H20). The single crystal PMN-PZT plate was parallel to the flat surface of the copper wire. If they were not parallel to each other, the amplitude of the receiving signal would be decreased, thus affecting the receiving response performance and decreasing the sensitivity of the needle hydrophone. Then the tube with copper wire and single crystal PMN-PZT plate were moved into a 40°C heater machine to reduce the

epoxy cure time. When the epoxy had cured, the copper and single crystal PMN-PZT plate were strongly bond together.

An adhesive layer of the non-conductive epoxy (EPO-TEK 301) was smeared around the copper wire at the junction of the single crystal PMN-PZT and copper wire. Since the copper wire is 2 mm long and the thickness of single crystal PMN-PZT plate is 0.31 mm, be careful enough not smearing the non-conductive epoxy on the other surface of the single crystal PMN-PZT plate. If the surface was smeared with the non-conductive epoxy, the positive electrode of the needle hydrophone would be failed, thus could not receive signals after fabricating. Since the size of the copper wire and the single crystal PMN-PZT were too small, the help of microscopy (I Cam Scope) was needed, including the next step. Several minutes after the non-conductive epoxy was dry, an adhesive of the conductive silver epoxy (EPO-TEK H20) was smeared from the surface of the PMN-PZT plate to the iron tube. Thus the two electrodes of the needle hydrophone had been made.

Table 4-1. Acoustic parameters of the matching layers used in fabrication.

	Z_1 [Mrayl]	V^D [m/s]	ρ [kg/m ³]	α [dB/mm/MHz]	t [mm]
1st layer	8.60	2375	3621	2.07	0.063
2nd layer	2.85	2015	1413	0.01	0.05

Then the two matching layers (Comico_11 and Comico_10, KoMiCo Company) bonded together with the single crystal PMN-PZT plate. The acoustic parameters of the matching layers used in the manufacture is shown in Table 4-

1. The acoustic impedance of first matching layer is $Z_1 = 8.60 \text{ Mrayl}$, $Z_2 = 2.85 \text{ Mrayl}$, which are quite close to the values in theory according to DeSilets et al. The two matching layers was bonded together with piezoelectric single crystal PMN-PZT by using epoxy (EPO-TEK 301).

Finally, the needle-head was connected to a 50_ coaxial cable for transmitting the signal to an amplifier. As the hydrophone was used under water, the connection between the needle-head and the coaxial cable was covered by silicone rubber to prevent ingress of water.

4-2. Characteristics evaluation

4-2-1. Receiving pulse-echo response

The performance of the PMN-PZT needle hydrophone was evaluated in a water tank. The experiment setup is shown in Fig.4-1. The PMN-PZT needle hydrophone was first characterized by examining its receiving response by using a plane transducer transmitting pulses. The PMN-PZT needle hydrophone was placed in a water tank of degassed water with the plane transducer placed at its bottom. The plane transducer was then excited with a function waveform generator (EZT DDF3010).

The PMN-PZT needle hydrophone was positioned for maximum received signal in the plane perpendicular to the transducer axis and measurements were made with the transducer excited by a 20-cycle tone burst with driving voltage in the frequency range of 0~10 MHz. The hydrophone output signal was measured over the region of the tone burst for which a voltage waveform of

constant amplitude was observed using an oscilloscope (LeCroy wave runner) and amplified with the Gain = 20 dB.

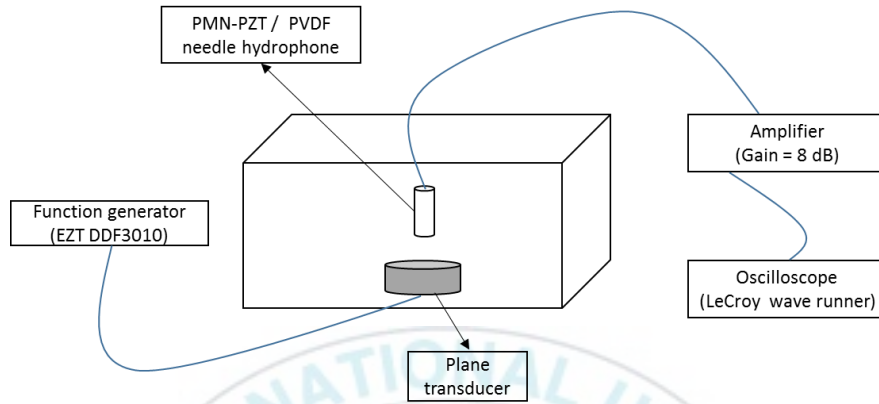


Fig.4-1. Schematic diagram of the setup for evaluation of the PMN-PZT needle hydrophone

In order to evaluate the performance of the fabricated PMN-PZT needle hydrophone, we made a comparison of the receiving waveforms and sensitivity with a standard commercial PVDF needle hydrophone (Precision Acoustic Ltd.) with the diameter of 0.2 mm. This time, two NDT transducers (Olympus) with the center frequency of 5.0 MHz and 7.5 MHz respectively were used as projectors for transmitting ultrasonic waves in the water. Since the system of the commercial PVDF needle hydrophone has an inherent Gain=8 dB, as a comparison, we used the PMN-PZT needle hydrophone placed at the same position and using the same procedure to measure the amplitude of the receiving signal with a matched amplifier (Gain = 8 dB).

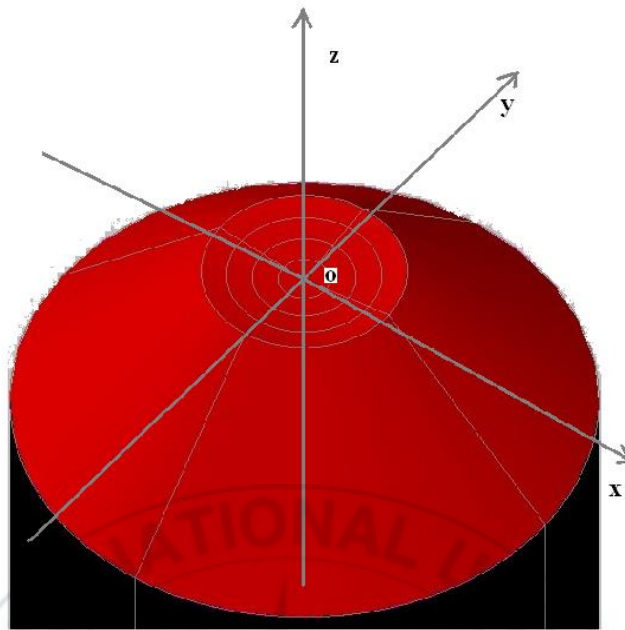


Fig.4-2. xyz rectangular coordinate system and the transducer

In this work, the acoustic field is analyzed with the help of xyz rectangular scanning system. As shown in Fig.4-2, the vertex of the concave is supposed as the origin point 0 and the xy plane is parallel to the circle plane of the transducer. So the wave is propagating along the z-axis. The positions in calculations and figures are related to this coordinate system.

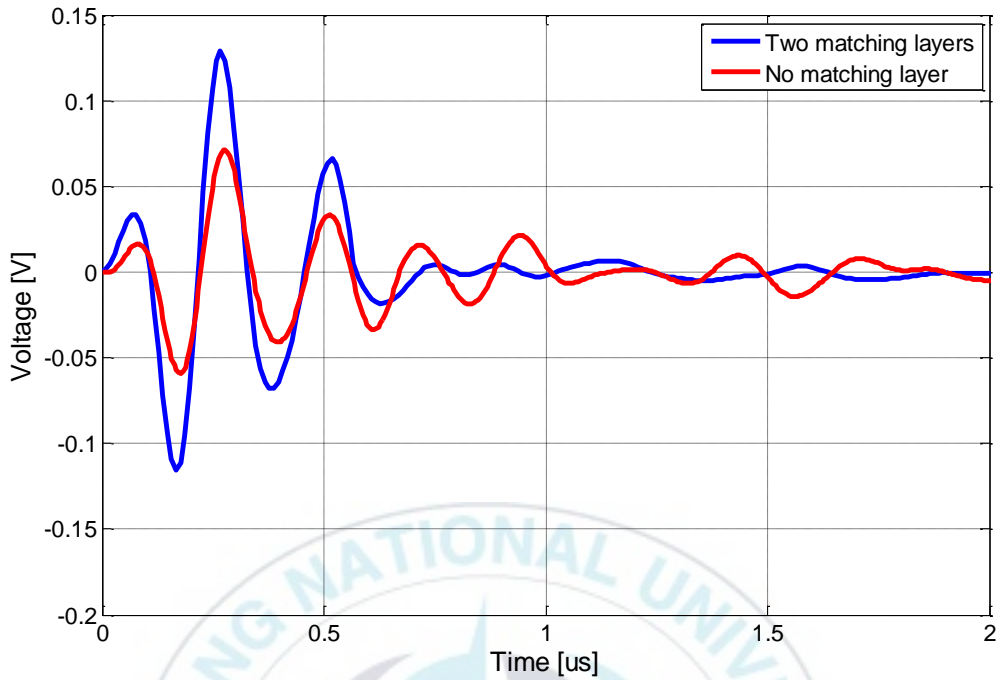


Figure 4-3. Wave graphs of the PMN-PZT without and with two matching layers (Attenuation=0, Gain=20dB)

As shown in Fig.4-3, the amplitude of the signal received by the PMN-PZT needle hydrophone with two matching layers is about 2 times higher than that received by the PMN-PZT needle hydrophone without matching layer. After adding the two matching layers (Comico_11 and Comico_10 with the acoustic impedance $Z_1 = 8.60 \text{ Mrayl}$ and $Z_2 = 2.85 \text{ Mrayl}$, respectively), the surface reflection of the ultrasonic waves is greatly decreased. Thus increasing the ultrasonic intensity received by the PMN-PZT needle hydrophone. While without matching layers, since the existence of the mismatch of the acoustic impedance between water and single crystal PMN-PZT, some of the ultrasonic intensity is reflected on the surfaces. That is why small amplitude of the signal

is received.

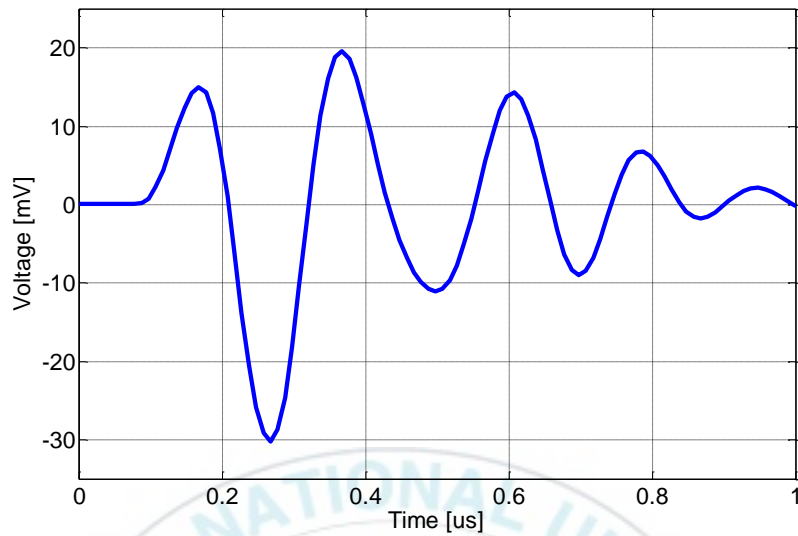


Fig.4-4 Wave graph of the PMN-PZT needle hydrophone without an amplifier

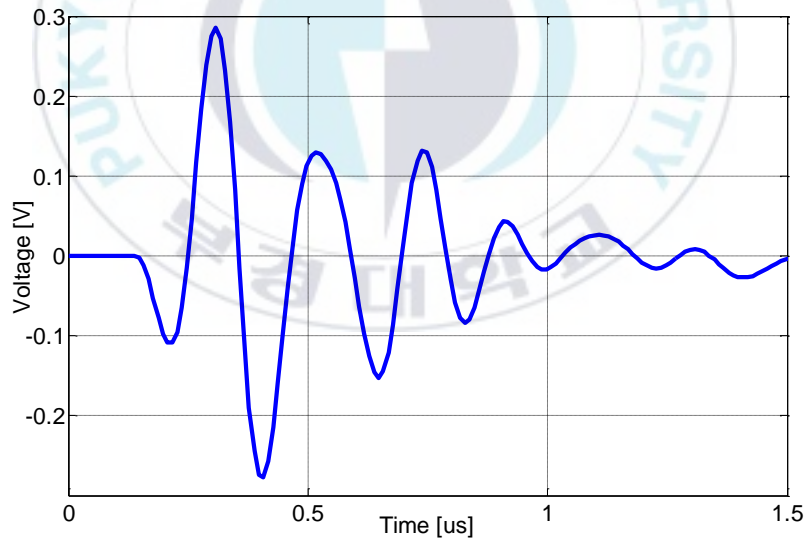


Fig.4-5. Wave graph of the PMN-PZT needle hydrophone with an amplifier

Fig.4-4 and Fig.4-5 show the receiving response of PMN-PZT needle hydrophones without and with an amplifier, respectively. In Fig.4-4, the peak-

to-peak amplitude of the signal is about 50mV, while in Fig.4-5 the peak-to-peak amplitude is amplified to about 550 mV with an amplifier (ZFL-500-BNC, Mini-circuit) showed in Fig.4-6. The Gain of the amplifier is about 20dB when the input voltage is 15V. And Fig.4-7 shows the receiving response of the PVDF needle hydrophone with an amplifier. The peak-to-peak amplitude is only about 19 mV, much shorter than the PMN-PZT needle hydrophone.



Fig.4-6 The mini-circuit ZFL-500-BNC amplifier

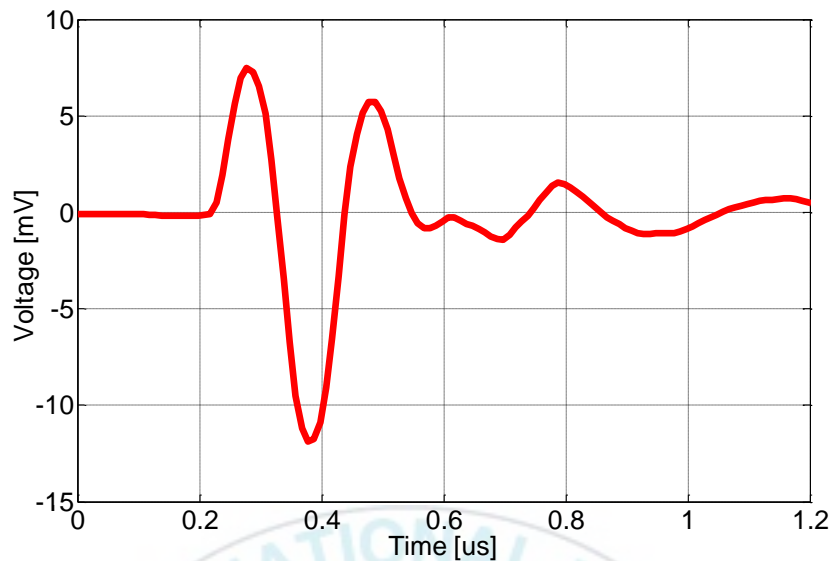


Fig.4-7.Wave graph of the PVDF needle hydrophone with an amplifier

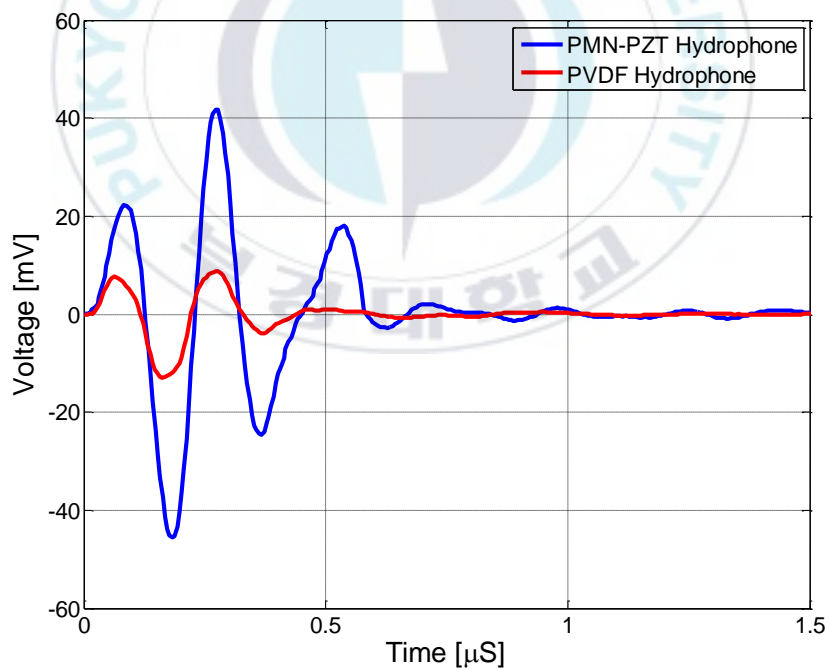


Fig.4-8. Comparison of waveform of typical signals for the PMN-PZT and PVDF needle hydrophones. (Attenuation=0, Gain=8dB)

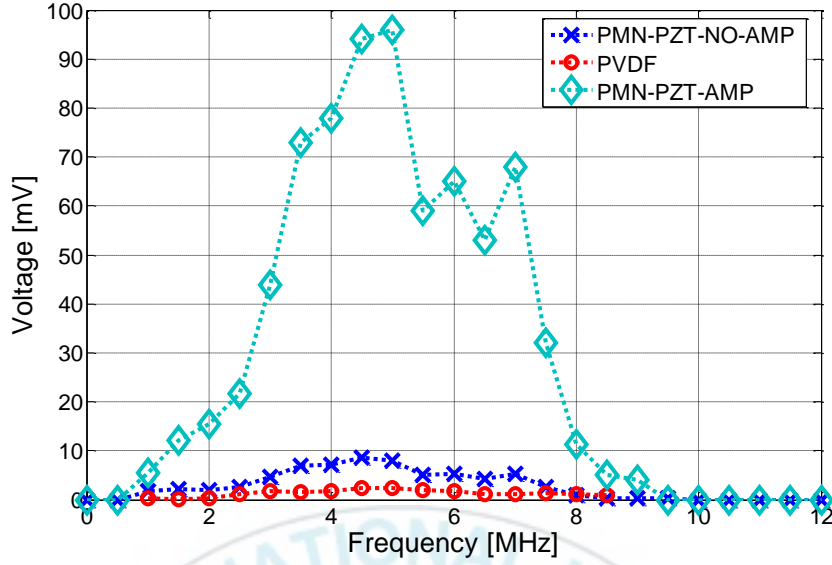


Fig.4-9. Comparison of amplitude variation according to frequency for the PMN-PZT and PVDF needle hydrophones. (Attenuation=0, Gain=8dB)

As an example, Fig.4-8 shows the waveform and spectrum of the received signals when the projector is a plane transducer with the center frequency of 5 MHz. From the waveform, we can see that the amplitude of the signal received by the PMN-PZT needle hydrophone is much bigger than that received by the standard commercial PVDF needle hydrophone. Fig.4-9 shows the comparison of the amplitude of measured signals according to different frequencies of transmitting ultrasonic signals. From 1~6 MHz, the projector is a plane transducer with the center frequency of 5 MHz, while after 6 MHz, the projector is a plane transducer with the center frequency of 7.5 MHz. It is shown that, compared with the standard commercial PVDF needle hydrophone, the fabricated PMN-PZT needle hydrophone has much higher sensitivity in the frequency range of 1~10 MHz.

Fig.4-10 shows the photograph of the fabricated needle hydrophone. The

iron probe of the needle hydrophone is about 2.5 cm long and the diameter of the thick copper tube is 1 cm. The single crystal PMN-PZT and the two matching layers locate to the tip of the iron probe. Because of the small size ($0.5 \times 0.5 \text{ mm}^2$ in area), they could not be seen clearly.



Fig.4-10. Photograph of the fabricated PMN-PZT needle hydrophone

4-2-2. Discussion

The results of the comparison between the fabricated PMN-PZT needle hydrophone and the standard commercial PVDF needle hydrophone adequately illustrate that single crystal PMN-PZT has ultra-high piezoelectric properties and will promote the development of the needle hydrophone when used as the sensing material.

However, it should be recognized that the sensitivity of the fabricated PMN-PZT needle hydrophone in the range of 0~10 MHz is not as stable and flat as the

result obtained from the piezoCAD simulation. This may result from the fabrication process, such as there is a small angle between the PMN-PZT single crystal plate and the copper tube surface, etc. The problems will found out and solved in the future work.



Ch. 5. Photoacoustic imaging by the fabricated PMN-PZT needle hydrophone

5-1. Photoacoustic imaging system

5-1-1. Indocyanine green (ICG) specimen

Indocyanine green (ICG) is a cyanine dye used in medical diagnostics. It is used for determining cardiac output, hepatic function, and liver blood flow, and for ophthalmic angiography. It has a peak spectral absorption at about 800 nm. These infrared frequencies penetrate retinal layers, allowing ICG angiography to image deeper patterns of circulation than fluorescein angiography. ICG binds tightly to plasma proteins and becomes confined to the vascular system. ICG has a half-life of 150 to 180 seconds and is removed from circulation exclusively by the liver to bile juice.

ICG, a tricyanocyanine dye with peak absorption at almost 800 nm, has been used as a diagnostic aid for measuring blood volume, cardiac output, or hepatic function. Noninvasive photoacoustic angiography of animal brains has been reported with ICG [43]. When it is injected into the circulation system of a rat, ICG significantly enhances the absorption contrast between the blood vessels and the background tissues. Because near-infrared light can penetrate deep into brain tissues through the skin and the skull, the vascular distribution in the rat brain was successfully reconstructed from the photoacoustic signals with high spatial resolution and low background. Subsequently, it was reported that PAT could image objects embedded at depths of up to 5 cm at a resolution of <1 mm

with a sensitivity of <10 pM of ICG in the blood [44]. The resolution was found to deteriorate slowly with increasing imaging depth.

In this experiment, the ICG was mixed together with some water to make ICG solution. And then the ICG solution was insulated into a silicon tube with the outer diameter of 2mm. Fig.5-1 shows the ICG specimen fixed on a rectangular plastic. The center part of the silicon tube was scanned with the PAI system.

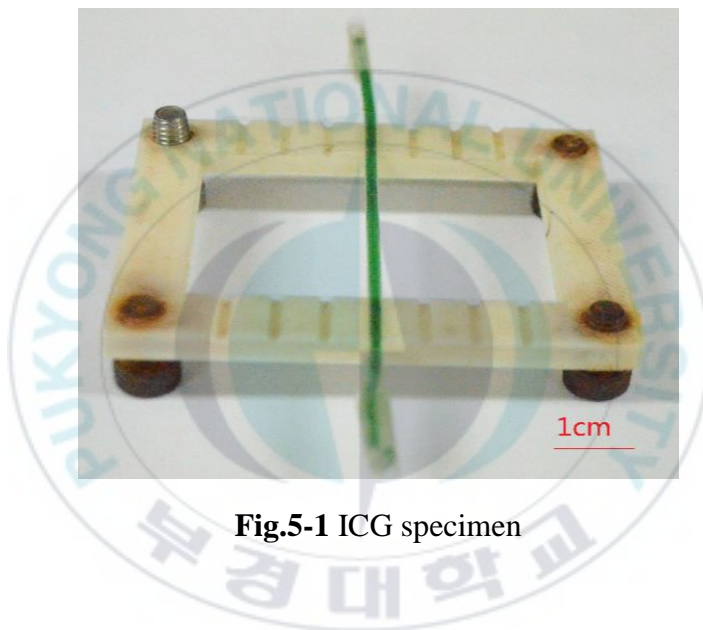


Fig.5-1 ICG specimen

5-1-2. Photoacoustic imaging system

In our US-based integrated photoacoustic imaging system (Fig.5-2), the pulsed Q-switched Nd:YAG laser was used as the PA signal excitation source. The free space laser output was focused by an objective lens and coupled led into an optical fiber for delivery. The light delivery system was combined with the fabricated PMN-PZT needle hydrophone and they were fastened on the XY moving stage controller and moved at the same time when scanning the ICG specimen. The ICG sample was immersed and fixed in the bottom of a water

tank. The circumferential scanning (B-scan) was accomplished by the X-Y direction moving stage controller. The laser pulse and PMN-PZT needle hydrophone unit were used to generate US pulses and receive PA waves, respectively. For each rectangular B scan, 200 time-resolved PA signals (A-lines) was recorded. The received PA signals was amplified by 20 dB through an amplifier (ZFL-500-BNC, Mini-circuit), and then digitized and processed by a NI PXI-10420 (National Instruments). At last, after data processing with MATLAB, the PA image of ICG specimen was acquired.



Fig.5-2. PAI system

5-2. PAI results

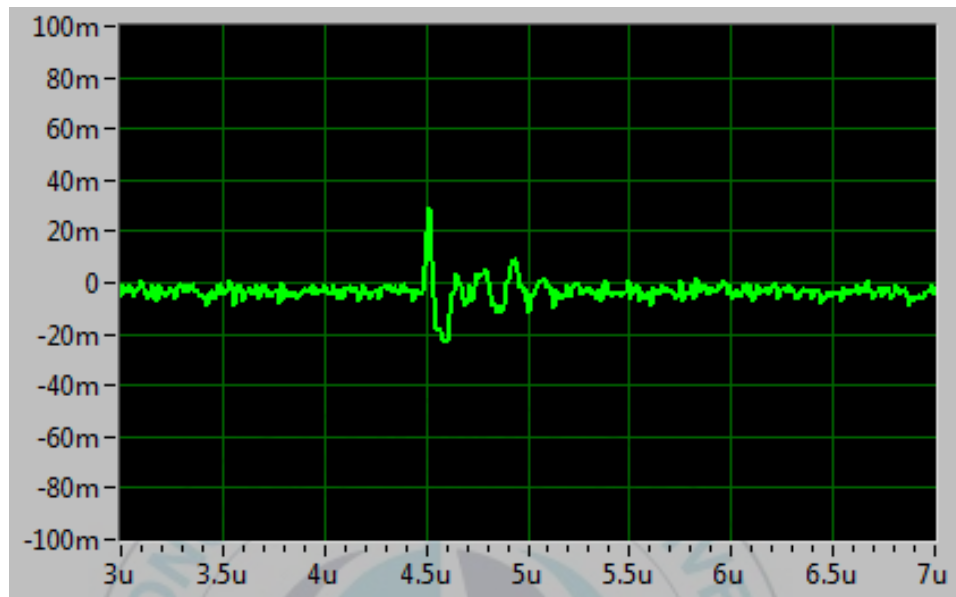


Fig.5-3 PA signal of PMN-PZT needle hydrophone without an amplifier

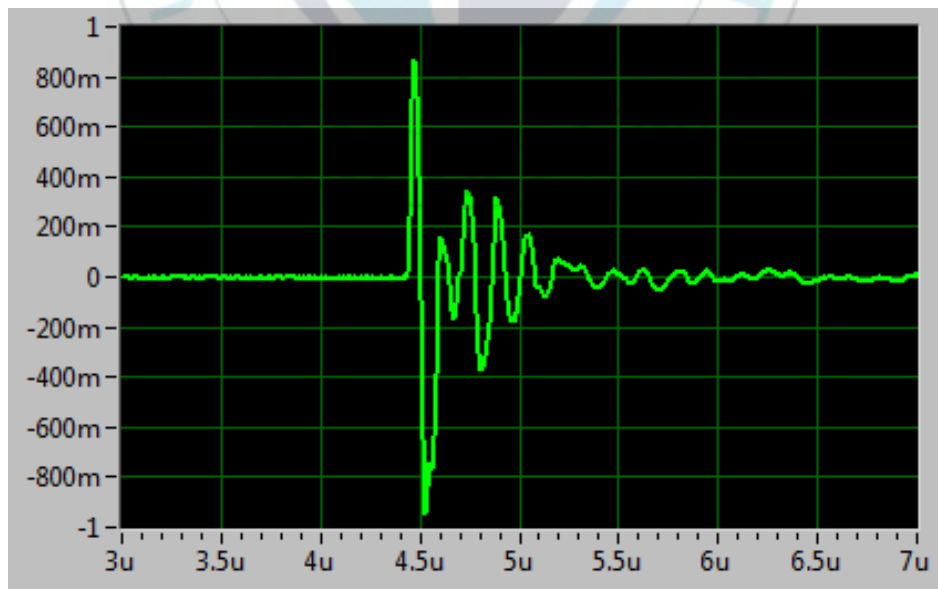


Fig.5-4 PA signal of PMN-PZT needle hydrophone with an amplifier (20dB)

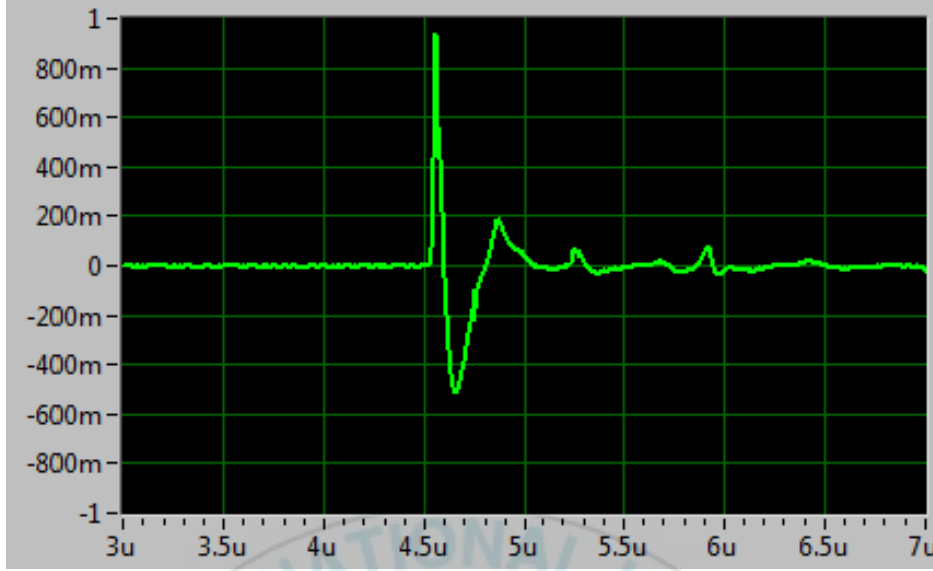


Fig.5-5 PA signal of PVDF needle hydrophone with an amplifier (Gain=34dB)

Fig.5-3 and Fig.5-4 show the received photoacoustic signals of the PMN-PZT needle hydrophone without and with an amplifier (Gain=20dB), respectively. In Fig.5-3, the peak-to-peak amplitude of the photoacoustic signal is about 50mV, while in Fig.5-4, with the amplifier, the peak-to-peak amplitude is about 1.8V. In order to evaluate the characteristics of the PMN-PZT needle hydrophone, the amplitude of the photoacoustic signal is compared with a commercial PVDF needle hydrophone under the same condition. And in Fig.5-5, the peak-to-peak amplitude of the photoacoustic signal received by the PVDF needle hydrophone is about 1.4V with the Gain=34dB. From the comparison, it is concluded that the PMN-PZT needle hydrophone has much higher sensitivity than the commercial PVDF needle hydrophone. And the results confirmed the simulation results of the peizoCAD.

Fig.5-6 and Fig.5-7 show the PA image of the ICG and human hair specimens, respectively. The golden line in the graph are the ICG solution and

human hair. The PA images of ICG and human hair specimens show high resolution and high contrast. This demonstrate that the fabricated PMN-PZT needle hydrophone has a high sensitivity and can be used as ultrasound probes for PAI.

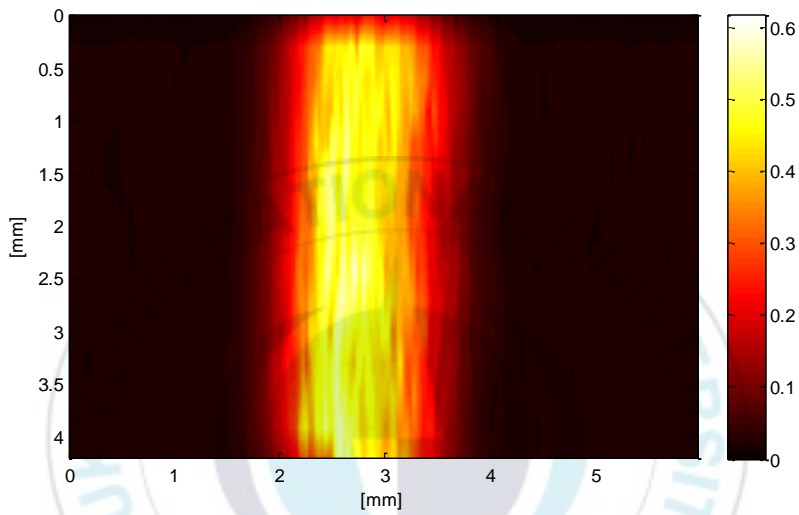


Fig.5-6 Photoacoustic image of ICG specimen

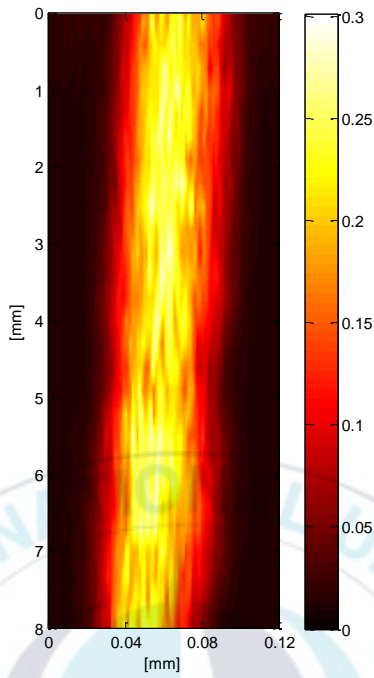


Fig.5-7 Photoacoustic image of human hair specimen

Ch. 6. Conclusions

In this thesis, we have designed and fabricated a new type of needle hydrophone with high sensitivity and wide bandwidth in the range of 1~10 MHz is described in detail. The sensitive part is a small size ($0.5 \times 0.5 \text{ mm}^2$) lead magnesium niobate-lead titanate (PMN-PZT) single crystal material with two matching layers on the tip of the needle. The experiment result shows that the amplitude of the signal received by the PMN-PZT needle hydrophone with two matching layers is about 2 times higher than that received by the PMN-PZT needle hydrophone without matching layer.

Construction and performance of the PMN-PZT needle hydrophone are compared with other types of needle hydrophones. The receiving frequency responses of the hydrophones are estimated by the PiezoCAD program based on KLM model. The PMN-PZT needle hydrophone has been characterized to be more sensitive and has much more flat and stable frequency bandwidth than a PVDF needle hydrophone of the similar structure, and it is confirmed by the experiment.

Furthermore, using this fabricated PMN-PZT needle hydrophone, we established an Acoustic Needle Imaging System for low frequency photoacoustic imaging to get some images of specimen. It is shown that the photoacoustic images of the ICG specimen obtained by the system have high resolution and high contrast.

In conclusion, compared with conventional piezoelectric materials, Lead magnesium niobate-lead titanate (PMN-PZT) single crystal has ultra-high piezoelectric properties and extremely good dielectric and piezoelectric

properties as a result of enhanced polarizability arising from the coupling between two equivalent energy states. This single crystal can be used to fabricate high performance needle hydrophone and ultrasound transducers used for low frequency photoacoustic imaging.



References

- [1] Stephan Behrens, Konstantinos Spengos, Transcranial ultrasound-improved thrombolysis: diagnostic vs. therapeutic ultrasound, *Ultrasound in Medicine & Biology*, December 2001, Pages 1683–1689
- [2] Park, Seung-Eek, Characteristics of relaxor-based piezoelectric single crystals for ultrasonic transducers, *Ultrasonics, Ferroelectrics, and Frequency Control*, IEEE, Sept. 1997, 1140 - 1147
- [3] Jean-Michel Kiat, Yoshiaki Uesu, Monoclinic structure of unpoled morphotropic high piezoelectric PMN-PT and PZN-PT compounds, *Phys. Rev. B* 65, 064106, 17 January 2002
- [4] Ritter, T, Single crystal PZN/PT-polymer composites for ultrasound transducer applications, *Ultrasonics, Ferroelectrics, and Frequency Control*, IEEE, July 2000, 792 - 800
- [5] Vladimír Koval, Effect of PMN modification on structure and electrical response of x PMN–(1– x)PZT ceramic systems, *Journal of the European Ceramic Society*, June 2003, Pages 1157–1166
- [6] S. Jiansirisomboon, Mechanical properties and crack growth behavior in poled ferroelectric PMN–PZT ceramics, *Current Applied Physics*, June 2006, Pages 299–302
- [7] Maxime P. Look, Wim L. J. van Putten, Pooled Analysis of Prognostic Impact of Urokinase-Type Plasminogen Activator and Its Inhibitor PAI-1 in 8377 Breast Cancer Patients, *JNCI J Natl Cancer Inst* (2002) 94 (2), 116-128

- [8] Krishnan Sriram, Evidence for generation of oxidative stress in brain by MPTP: in vitro and in vivo studies in mice, Brain Research, February 1997, Pages 44–52
- [9] Kruger, R.A, Thermoacoustic computed tomography of the breast at 434 MHz, Microwave Symposium Digest, 1999 IEEE MTT-S International, 13-19 June 1999, 591 - 594
- [10] J. Chen, A. Shurland, J. Perry, B. Ossmann, T.R. Gururaja, in: Proceedings of the 10th IEEE International Symposium on Applications of Ferroelectrics, East Brunswick, NJ, USA, 18-21 August 1996, pp. 27-30.
- [11] Q.R. Yin, J.W. Fang, H.S. Luo, G.R. Li, in: Proceedings of the 12th IEEE International Symposium on Applications of Ferroelectrics, Honolulu, Hawaii, USA, 21 July-2 August 2000, pp. 569-572 Chapter 2
- [12] Xiaoning Jiang, Jinwook Kim and Kyugrim Kim. Relaxor-PT Single Crystal Piezoelectric Sensors. Crystals 2014, 4, 351-376
- [13] Sherman, C.H.; Butler, J.L. Transducers and Arrays for Underwater Sound; Springer: New York, NY, USA, 2007.
- [14] Haun, M.; Newnham, R. An experimental and theoretical study of 1–3 and 1–3–0 piezoelectric PZT-polymer composites for hydrophone applications. Ferroelectrics 1986, 68, 123–139.
- [15] Smith, W.A. Modeling 1–3 composite piezoelectrics: Hydrostatic response. IEEE Trans. Ultrason. Ferroelectr. Freq. Control 1993, 40, 41–49.
- [16] G. Gautschi. ‘Chapter 2: Piezoelectric sensorics: Force, Strain, Pressure,

Acceleration and Acoustic Emission Sensors, Materials and Amplifiers.’
Published by Springer, ISBN-3540422595(HB), p.6-7.

- [17] Ye. Bormashenko, R. Pogreb, Vibrational spectrum of PVDF and its interpretation, Polymer Testing, October 2004, Pages 791–796
- [18] E. Fukada. ‘History and recent progress of piezoelectric polymer research.’
in proc. 1998 IEEE Ultrason.Symp.,sendai, Japan, p.597-605.
- [19] E. Fukada. ‘History and recent progress in piezoelectric polymer research,’
IEEE Trans. Ultrason., Ferroelect. Freq. Contr., 2000, 171(1-4), p.1277-1290.
- [20] Koga Keiko, OhigashiHiroji. ‘Piezoelectricity and related properties of vinylidene fluoride and trifluoroethylene copolymers,’ Journal of Applied Physics, 1986, 59(6), p.2142-2150.
- [21] Long Wu, Chung-Chuang Wei, Tien-Shou Wu and Hsi-Chuan Liu.
‘Piezoelectricproperties of modified PZT ceramics.’Journal of Physics C: Solid State Physics, 1983, 16, p.2813-2821.
- [22] Gene H. Haertling, Ferroelectric Ceramics: History and Technology,
Journal of the American Ceramic Society, pages 797–818, April 1999
- [23] Warren P. Mason, Piezoelectricity, its history and applications, J. Acoust. Soc. Am. 70, 1561 (1981)
- [24] Knspik, D.A, A 100-200 MHz ultrasound biomicroscope, Ultrasonics, Ferroelectrics, and Frequency Control, IEEE, Nov. 2000, 1540 - 1549
- [25] Stephen J. Martin, Victoria Edwards Granstaff, Gregory C. Frye.
‘Characterization of a quartz crystal microbalance with simultaneous mass

and liquid loading.’ Anal. Chem., 1991, 63, p.2272-2281.

- [26] Yamanouchi Kazuhiko, Shibayama Kimio. ‘Propagation and Amplification of Rayleigh Waves and Piezoelectric Leaky Surface Waves in LiNbO₃.’ Journal of Applied Physics, 1972, 43(3), p.856-862
- [27] Hutson, A. R. ‘Piezoelectric Scattering and Phonon Drag in ZnO and CdS.’ Journal of Applied Physics, 1961, 32(10), p.2287-2292.
- [28] Jae-Hwan Park, Juyoung Park, Jae-Gwan Park, Byung-Kook Kim and Yoonho Kim. ‘Piezoelectric properties in PMN–PT relaxor ferroelectrics with MnO₂ addition.’ Journal of the European Ceramic Society, 2001, 21(10-11), p.1383-1386.
- [29] Sitti M, Campolo D, Yan J, Fearing R.S. ‘Development of PZT and PZN-PT based unimorph actuators for micromechanical flapping mechanisms.’ Robotics and Automation, 2001, 4, p.3839-3846.
- [30] Koichi Yokosawa, Ryuichi Shinomura, A 120-MHz Ultrasound Probe for Tissue Imaging, Ultrasonic Imaging, October 1996, 231-239
- [31] K. Martin, Rapid propagation of *Holostemma adakodien* Schult., a rare medicinal plant, through axillary bud multiplication and indirect organogenesis, Plant Cell Reports, 2002-08-01, pp 112-117
- [32] S.T. Lau, K.H. Lam, Piezoelectric PMN-PT fibre hydrophone for ultrasonic transducer calibration, Applied Physics A, January 2005, pp 105-110
- [33] Qifa Zhou, PMN-PT single crystal, high-frequency ultrasonic needle transducers for pulsed-wave Doppler application, Ultrasonics, Ferroelectrics,

and Frequency Control, IEEE, March 2007, 668 - 675

- [34] Zhi-Wen Yina, Hao-Su Luo, Growth, characterization and properties of relaxor ferroelectric PMN-PT single crystals, *Ferroelectrics*, 1999, 207-216
- [35] Shiroh Saitoh, Takashi Takeuchi, An Improved Phased Array Ultrasonic Probe Using 0.91 Pb(Zn_{1/3}Nb_{2/3})O₃–0.09PbTiO₃ Single Crystal, *Japanese Journal of Applied Physics*, 1999, 38 3880
- [36] S. Jiansirisomboon, Mechanical properties and crack growth behavior in poled ferroelectric PMN–PZT ceramics, *Current Applied Physics*, June 2006, Pages 299–302
- [37] Wang LV. 2008. Prospects of photoacoustic tomography. *Med Phys* 35: 5758–5767.
- [38] Xu M, Wang LV. 2006. Photoacoustic imaging in biomedicine. *Rev Sci Instrum* 77: 10.1063/1.2195024
- [39] YANG Di-Wu, ZHOU Zhi-Bin, Photoacoustic Imaging of Animals with an Annular Transducer Array, *CHIN. PHYS. LETT.* Vol. 31, No. 7 (2014) 074301
- [40] Diwu Yang, Da Xing, Fast full-view photoacoustic imaging by combined scanning with a linear transducer array, *Optics Express* Vol. 15, Issue 23, (2007) pp. 15566-15575
- [41] Shriram Sethuraman, Intravascular Photoacoustic Imaging Using an IVUS Imaging Catheter, *IEEE, transactions on ultrasonics, ferroelectrics, and frequency control*, vol. 54, no. 5, may 2007: 978-985

- [42] C. S. DeSilets, J. D. Fraser, G. S. Kino, IEEE Trans. Sonics and Ultrasonics, Vol. 25(3), pp. 115-125, 19
- [43] Wang X, Ku G, Wegiel MA, Bornhop DJ, Stoica G, Wang LV. 2004. Noninvasive photoacoustic angiography of animal brains in vivo with near-infrared light and an optical contrast agent. Opt Lett 29: 730–732
- [44] Ku G, Wang LV. 2005. Deeply penetrating photoacoustic tomograph in biological tissues enhanced with an optical contrast agent. Opt Lett 30: 507–509.



Acknowledgements

I would like to express my deepest gratitude to my advisor Dr. Junghwan Oh, Professor, Department of Interdisciplinary Program of Biomedical Mechanical & Electrical Engineering for his invaluable guidance, support and encouragement towards the completion of the experiments and writing of this thesis. Dr. Oh led me to the science world of the Biomedicine, and gave me the fundamentals knowledge of the acoustics and photoacoustics. I benefited a lot from his learning. Also, a great thank should be said to him for his selfless offer. And due to his care, my life in Korea is favoring.

I wish to thank the following professors, Dr. Kang-Lyeol Ha, Department of Physics and Dr. Kong, department of Biomedicine engineering. They are my familiar professor and taught me in the past two years. Their learning and kindness are very impressive. Especially Dr. Kang-Lyeol Ha, he taught me a lot about the acoustics and helped me a lot during doing the experiment and writing this thesis. I would like to say thanks to him.

I also have to say thanks to my schoolmates, Quang, Kyukyu, Dr. Hyun-ok Oh, Dr. Han-Su Suh and Dr. Yonggang Cao. Because they have helped me a lot in my study and living in PKNu. They shared their experience of the research and language study with me, selflessly. And it is a wonderful time to study and discuss with them. Thanks to the students and friends, Peiqing Cai, Lili Wang and so on, for their help and accompanying.

I am grateful to my parents and my brother for their unending love, sustained support and encouragement during these years when I left home.